Computers and Mathematics with Applications 70 (2015) 1887–1905

Contents lists available at ScienceDirect

Computers and Mathematics with Applications

journal homepage: www.elsevier.com/locate/camwa

On a dissolution–diffusion model. Existence, uniqueness, regularity and simulations

María Emilia Castillo [a,b,*], Pedro Morin [a,c]

[a] Instituto de Matemática Aplicada del Litoral (IMAL), Universidad Nacional del Litoral and CONICET, Argentina
[b] Departamento de Matemática, Facultad de Humanidades y Ciencias, Universidad Nacional del Litoral, Argentina
[c] Departamento de Matemática, Facultad de Ingeniería Química, Universidad Nacional del Litoral, Argentina

ARTICLE INFO

Article history:
Received 7 November 2014
Received in revised form 17 April 2015
Accepted 1 August 2015
Available online 11 September 2015

Keywords:
Dissolution–diffusion
Drug release
Partial differential equations
Finite elements

ABSTRACT

We perform a mathematical analysis of a model for drug dissolution–diffusion in non erodible nor swellable devices. We deduce a model and obtain a coupled nonlinear system which contains a parabolic equation for the dissolved drug and an ordinary differential equation for the solid drug, which is assumed to be distributed in the whole domain into microspheres which can differ in size. We analyze existence, uniqueness, and regularity properties of the system. Existence is proved using Schauder fixed point theorem. Lack of uniqueness is shown when the initial concentration of dissolved drug is higher than the saturation density in a region, and uniqueness is obtained in the non-saturated case. A square root function appears in the equation for the solid drug, and is responsible for the lack of uniqueness in the oversaturated case. The regularity results are sufficient for the optimal a priori error estimates of a finite element discretization of the system, which is presented and analyzed here. Simulations illustrating some features of the solutions and a good agreement with laboratory experiments are presented. Finally, we obtain error estimates for the finite element method used to compute the simulations.

1. Introduction

Numerous mathematical approaches have been proposed to give an adequate theoretical background to the modeling of drug release from polymeric devices [1,2]. The interest in this kind of systems has increased in the medical and pharmaceutical industry, because controlled drug-release systems allow for predictable release kinetics, small fluctuations of plasma drug level, diminishing the amount of toxic secondary effects, among other advantages [3,4]. A precise application is a progesterone-releasing intravaginal device called CIDR (Controlled Internal Drug Release, InterAg Manufacturing, New Zealand) depicted in Fig. 1. This is an intravaginal progesterone insert used in the beef cattle, dairy cattle, goat and sheep industries, to release the progesterone at a controlled rate into the bloodstream. In all species, CIDRs are used for the synchronization of estrus, which can be highly beneficial in large herds because groups of cows and heifers can be bred at the same time in a narrow window, achieving a higher pregnancy rate and precise calving dates [5,6].

We focus here on a model based on a diffusion equation including a continuous dissolution source described by the Noyes–Whitney equation; other models are based on a moving dissolution front separating a region of coexisting solid and dissolved drug from a region of completely dissolved drug; see [7,8] for a detailed description of other models.

* Correspondence to: IMAL — CCT CONICET Santa Fe, Colectora Ruta Nac. 168, Paraje El Pozo, 3000 Santa Fe, Argentina.
E-mail addresses: mecastillo@santafe-conicet.gov.ar (M.E. Castillo), pmorin@santafe-conicet.gov.ar (P. Morin).

http://dx.doi.org/10.1016/j.camwa.2015.08.004
0898-1221/

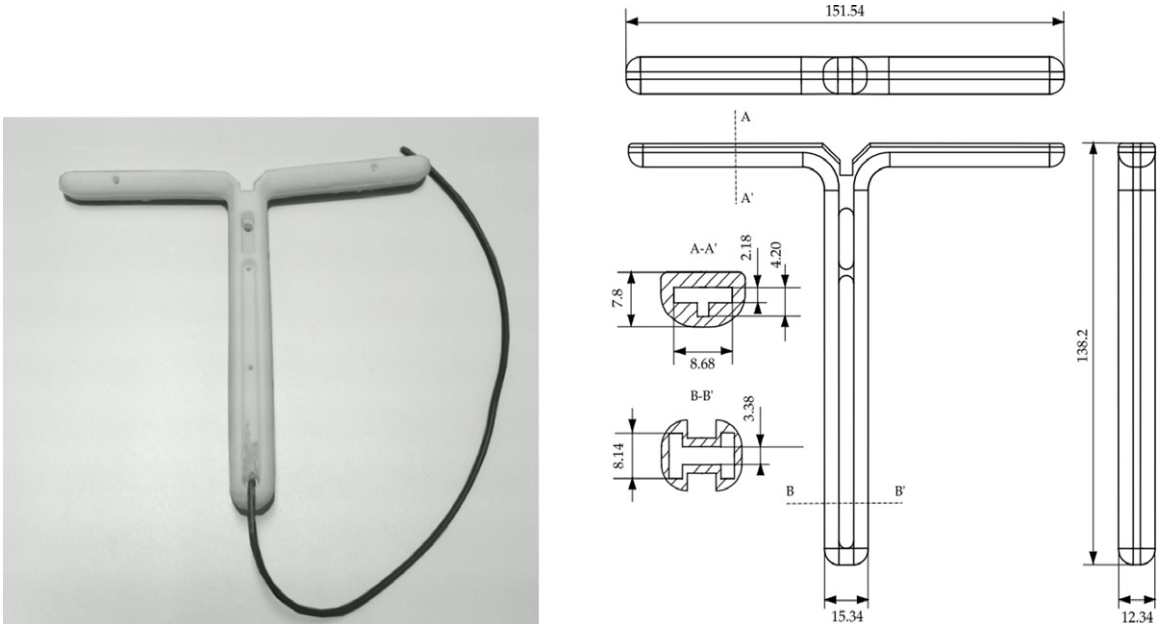

Fig. 1. CIDR device (InterAg Manufacturing, New Zealand). Photograph (left) and scheme (right). The inner structure can be observed through transversal cuts denoted by A–A′ and B–B′. Lengths are measured in millimeters.

Up to now, all mathematical studies have consisted in finding exact solutions for simple geometries using Fourier analysis, or simplified quasi-stationary assumptions, such as fast or slow dissolution rates relative to the diffusion of the already dissolved drug; which are not realistic in many situations (see [9] and references therein). The goal of this article is to study qualitative as well as quantitative properties of a dissolution–diffusion problem modeling the kinetics of a drug inside a polymeric device, avoiding the assumption of fast or slow dissolution rate relative to the diffusion. We want to avoid this kind of assumption to have a model with a wider range of applicability, since there is a large variety of polymers and drugs, which are combined to design drug-releasing devices [4].

We first prove existence of solutions, and study uniqueness and regularity properties. Secondly, we propose and analyze an algorithm for the numerical approximation of the solutions, where the regularity estimates are instrumental for obtaining optimal a priori error estimates. The numerical approximations allow us to visualize the behavior of the solutions and compute some measurable quantities with a striking agreement to laboratory experiments performed on CIDR devices.

The rest of the article is organized as follows. In Section 2 we deduce the mathematical model and prove existence of solutions in Section 3. Uniqueness of solutions is discussed in Section 4 where uniqueness is proved under the assumption that the initial concentration of dissolved drug is less than or equal to the maximum solubility, and the existence of multiple solutions is proved in a situation where the initial concentration of dissolved drug is above saturation. In Section 5 regularity estimates are obtained for both state variables, concentration of dissolved drug C and area of solid particles per unit volume a. In Section 6 we propose a finite element discretization and show some numerical results, which illustrate on the regularity of the solutions and the good agreement with laboratory experiments. Finally, in Section 7 we prove optimal a priori estimates for the proposed time–space discretization. We end this article with a concluding section summarizing our contributions and discussing potential future work.

2. Mathematical model and weak formulation

We start this section by briefly deducing a model for drug dissolution–diffusion in a non-erodible polymeric device. We consider a model for one drug, which can be either in a solid or in a dissolved state. We assume that the solid drug is distributed in particles of equal density, dispersed throughout the whole device, which can differ in mass and volume, but keep a spherical shape when dissolved [7]. We also assume that these non-dissolved particles are so small that they do not affect the diffusion of the dissolved drug, which thus evolves by diffusion with constant coefficient.

Under these assumptions we can state the mathematical model on a domain $\Omega \subset \mathbb{R}^3$, occupied by the polymeric device. If C denotes the concentration of dissolved drug, following the same steps used to obtain the diffusion equation with Fick's law we arrive at the following equation:

$$\frac{\partial C}{\partial t} - D\Delta C = -\frac{\partial m}{\partial t}, \quad x \in \Omega,\ t > 0, \tag{2.1}$$

where D is the drug diffusion coefficient and m is the mass of solid drug per unit volume, so that $-\frac{\partial m}{\partial t}$ is the mass of solid drug being dissolved per unit volume per unit time.

Following [7], we use the Noyes–Whitney model for the dissolution of the microspheres, i.e., we assume that the microspheres dissolve at a rate proportional to the product of their surface area and the difference between the saturation solubility C_s and the concentration around them. If a denotes the area of the microspheres of solid drug per unit volume, this can be stated mathematically as

$$\frac{\partial m}{\partial t}(x,t) = -k_D a(x,t)(C_s - C(x,t)), \quad x \in \Omega,\ t > 0, \tag{2.2}$$

where k_D is the dissolution rate constant of the solid drug particles. Using relations between radius, area and mass of a sphere we can rewrite (2.2) as

$$\frac{\partial a}{\partial t} = -\underbrace{\frac{4k_D\sqrt{\pi}N^{1/2}}{\rho_s}}_{\beta}\sqrt{a}(C_s - C), \quad x \in \Omega,\ t > 0, \tag{2.3}$$

where N represents the number of particles per unit volume and ρ_s is the intrinsic density of the solid drug particles.

Statement of the problem. Adding initial conditions and boundary conditions of Neumann and Robin type we arrive at the following problem:

$$\begin{aligned}
\frac{\partial C}{\partial t} - D\Delta C &= k_D a(C_s - C), && \text{in } \Omega \times (0, t_F),\\
\frac{\partial a}{\partial t} &= -\beta\sqrt{a}(C_s - C), && \text{in } \Omega \times (0, t_F),\\
C &= C_0, && \text{in } \Omega \times \{0\},\\
a &= a_0, && \text{in } \Omega \times \{0\},\\
D\frac{\partial C}{\partial \mathbf{n}} &= 0, && \text{on } \Gamma_N \times (0, t_F),\\
D\frac{\partial C}{\partial \mathbf{n}} &= k_B(C_B - C), && \text{on } \Gamma_B \times (0, t_F).
\end{aligned} \tag{2.4}$$

This problem is stated over $\Omega \subset \mathbb{R}^d$ $(d = 1, 2, 3)$, which is an open, bounded and connected set with Lipschitz boundary $\Gamma = \Gamma_N \cup \Gamma_B$. Γ_B is the nontrivial part of the boundary where drug is released to the surrounding medium, and $\Gamma_N = \Gamma \setminus \Gamma_B$ is the insulated part; C_B denotes the drug concentration in the bulk medium, k_B the external mass transfer coefficient, $\frac{\partial C}{\partial \mathbf{n}} = \nabla C \cdot \mathbf{n}$ and $\mathbf{n}$ denotes the exterior unit normal to $\partial\Omega$. We assume also that

$$D, k_D, k_B, C_B \in (0, +\infty), \qquad \beta \in L^\infty(\Omega), \quad \beta \geq 0, \tag{2.5}$$

$$C_0, a_0 \in L^\infty(\Omega), \quad C_0, a_0 \geq 0. \tag{2.6}$$

Proceeding as usual, integrating by parts in Ω, we arrive at the following weak formulation of the problem.

Definition 1. The pair (C, a) is called a weak solution of (2.4) if $C \in L^2(0, t_F; H^1(\Omega))$, with $C_t \in L^2(0, t_F; H^{-1}(\Omega))$, $a \in H^1(0, t_F; L^2(\Omega))$ and

$$\begin{aligned}
\langle C_t(t), v\rangle + \mathscr{B}[C(t), v] &= k_D\int_\Omega a(t)(C_s - C(t))v + k_B C_B\int_{\Gamma_B} v, && \forall v \in H^1(\Omega),\ \text{a.e. } t \in (0, t_F)\\
\int_\Omega a_t(t)w &= \int_\Omega \beta(C(t) - C_s)\sqrt{a(t)}w, && \forall w \in L^2(\Omega),\ \text{a.e. } t \in (0, t_F)\\
C(0) &= C_0, \qquad a(0) = a_0,
\end{aligned} \tag{2.7}$$

where $\langle f, v\rangle$ stands for the evaluation of the functional $f \in H^{-1}(\Omega)$ in $v \in H^1(\Omega)$ and

$$\mathscr{B} : H^1(\Omega) \times H^1(\Omega) \to \mathbb{R}, \qquad \mathscr{B}[C, v] := D\int_\Omega \nabla C\nabla v + k_B\int_{\Gamma_B} Cv.$$

The space $L^2(\Omega)$ is the space of Lebesgue measurable functions on Ω which are square integrable, $H^1(\Omega)$ denotes the usual Sobolev space of functions in $L^2(\Omega)$ with weak derivatives of first order in $L^2(\Omega)$ and $H^{-1}(\Omega)$ denotes the dual space of $H^1(\Omega)$. The spaces $L^p(0, t_F; X)$ denote the usual spaces of weakly measurable functions $f : [0, t_F] \to X$, such that $\int_0^{t_F} \|f(t)\|_X^p\, dt < \infty$. The space $H^1(0, t_F; X)$ denotes the space of functions in $L^2(0, t_F; X)$ with weak derivative of first order in $L^2(0, t_F; X)$; see [10, Chapter 3] for details and main results.

Since we only consider weak solutions to (2.4), we will usually omit the word *weak* in the sequel.

Remark 2. The following Friedrich inequality holds for a constant $\mathbb{C}_F$ depending on Γ_B and Ω:

$$\|v\|^2_{L^2(\Omega)} \leq \mathbb{C}_F^2\left(\|\nabla v\|^2_{L^2(\Omega)} + \|v\|^2_{L^2(\Gamma_B)}\right), \quad \forall v \in H^1(\Omega). \tag{2.8}$$

As an immediate consequence of this and the trace theorem, the bilinear form $\mathscr{B}$ is coercive and bounded, i.e., there exist positive constants $\mathbb{C}_1, \mathbb{C}_2$ such that, for all $v, w \in H^1(\Omega)$,

$$\mathbb{C}_1\|v\|^2_{H^1(\Omega)} \leq \mathscr{B}[v, v] \quad \text{and} \quad \mathscr{B}[v, w] \leq \mathbb{C}_2\|v\|_{H^1(\Omega)}\|w\|_{H^1(\Omega)}. \tag{2.9}$$

These constants $\mathbb{C}_1, \mathbb{C}_2$ depend only on D, k_B, Γ_B and Ω.

3. Existence of solutions

In this section we prove the existence of solutions of (2.4) by using Schauder fixed point theorem. Problems with similar features have been studied in [11,12]. The proofs in [11] are based on a regularization of the non-Lipschitz term and the proofs from [12] are based on an iteration at the infinite-dimensional level. Even though the proofs of [11,12] could be adapted to our problem, we decided to include a new proof to make the article more self-contained. The main result of this section is stated at the end as Theorem 6.

3.1. Fixed point formulation

We notice that if C were known, an explicit formula for a could be obtained by solving an ordinary differential equation. More precisely, the following lemma holds, whose proof is trivial and is thus omitted.

Lemma 3. *If $C \in L^2(0, t_F; H^1(\Omega))$, $C_t \in L^2(0, t_F; H^{-1}(\Omega))$, $C(0) = C_0$ and*

$$\langle C_t(t), v\rangle + \mathscr{B}[C(t), v] = k_D \int_\Omega a(t)(C_s - C(t))v + k_B C_B \int_{\Gamma_B} v, \quad \forall v \in H^1(\Omega), \ \text{a.e. } t \in (0, t_F) \tag{3.1}$$

with

$$a(t) = \max\left\{0, \sqrt{a_0} + \frac{1}{2}\int_0^t \beta\,(C(\tau) - C_s)\,\mathrm{d}\tau\right\}^2, \quad \forall t \in [0, t_F], \tag{3.2}$$

then (C, a) is a weak solution of (2.4). In other words, if C is the weak solution of the (linear) diffusion problem

$$\begin{aligned}
\frac{\partial C}{\partial t} - D\Delta C + k_D a C &= k_D a C_s, && \text{in } \Omega \times (0, t_F),\\
C &= C_0, && \text{in } \Omega \times \{0\},\\
D\frac{\partial C}{\partial \mathbf{n}} &= 0, && \text{on } \Gamma_N \times (0, t_F),\\
D\frac{\partial C}{\partial \mathbf{n}} &= k_B(C_B - C), && \text{on } \Gamma_B \times (0, t_F),
\end{aligned} \tag{3.3}$$

with a satisfying (3.2), then (C, a) is a weak solution of (2.4).

In the following, we will prove the existence of C satisfying (3.1) resorting to Schauder fixed point theorem [13, Corollary 11.2, p. 280]. We define

$$\mathcal{B} = L^2(0, t_F; L^2(\Omega)),$$
$$\mathcal{G} = \{u \in \mathcal{B} : 0 \leq u \leq \bar{C}_0 \text{ for almost all } t \in [0, t_F] \text{ and almost all } x \in \Omega\},$$

with $\bar{C}_0 = \max\left\{\|C_0\|_{L^\infty(\Omega)}, C_s\right\}$ and notice that $\mathcal{G}$ is a closed convex subset of $\mathcal{B}$. Furthermore, we define the mapping $T : \mathcal{G} \to \mathcal{B}$ as follows: given $\tilde{C} \in \mathcal{G}$, we define a as

$$a(t) = \max\left\{0, \sqrt{a_0} + \frac{1}{2}\int_0^t \beta\left(\tilde{C}(\tau) - C_s\right)\,\mathrm{d}\tau\right\}^2, \tag{3.4}$$

and notice that $a \in L^\infty(0, t_F; L^\infty(\Omega))$, because (3.4) yields

$$0 \leq a \leq \left(\|a_0\|^{1/2}_{L^\infty(\Omega)} + \frac{1}{2}t_F\|\beta\|_{L^\infty(\Omega)}\bar{C}_0\right)^2 =: \bar{A}_0. \tag{3.5}$$

Finally, let $C = T(\tilde{C})$ be the weak solution of the linear diffusion equation (3.3) with a given by (3.4), which exists and is unique due to the basic theory for parabolic PDE [14]. Moreover, using standard arguments (as in [14, Section 7.1.2]) we obtain that

$$\|C\|^2_{L^2(0,t_F;H^1(\Omega))} + \|C_t\|^2_{L^2(0,t_F;H^{-1}(\Omega))} \leq \mathbb{C}_3\left(\|C_0\|^2_{L^2(\Omega)} + |\Omega|t_F\bar{A}_0 + k_B C_B^2|\Gamma_B|t_F\right), \tag{3.6}$$

with $\mathbb{C}_3$ depending only on D, k_B, k_D, C_s, C_B and $\mathbb{C}_F$.

In the next section we will prove the existence of the fixed point C of T and existence of weak solutions of (2.4) will follow from the next lemma, whose proof is also trivial and thus omitted.

Lemma 4. *If $C \in \mathcal{G}$ is a fixed point of T, i.e., $T(C) = C$, and a is given by (3.2), then (C, a) is a weak solution of (2.4).*

3.2. Existence of a fixed point

We have already noted that $\mathcal{G}$ is convex and closed in $\mathcal{B}$, which is one assumption of Schauder fixed point theorem [13, Corollary 11.2]. Recalling that for $\tilde{C} \in \mathcal{G}$, always $C := T(\tilde{C}) \in L^2(0, t_F; L^2(\Omega))$, the next proposition implies that $T(\mathcal{G}) \subset \mathcal{G}$, which is another assumption of the theorem.

Proposition 5. *Let $a \in L^\infty(0, t_F; L^\infty(\Omega))$ with $a \geq 0$, let $C_0 \in L^\infty(\Omega)$ with $C_0 \geq 0$, and let C be the weak solution of (3.3). Then $0 \leq C \leq \bar{C}_0 = \max\left\{\|C_0\|_{L^\infty(\Omega)}, C_s\right\}$ for almost all $x \in \Omega$ and almost all $t \in [0, t_F]$. Moreover, if $C_0 \geq C_B$, then $C \geq C_B$ for almost all $x \in \Omega$ and almost all $t \in [0, t_F]$.*

Proof. Setting $v = \left(C - \bar{C}_0\right)_+ := \max\{C - \bar{C}_0, 0\}$ in (3.1) and taking into account that we have defined the constant $\bar{C}_0$ as $\bar{C}_0 = \max\left\{\|C_0\|_{L^\infty(\Omega)}, C_s\right\}$, we obtain the following equality:

$$\left\langle \left(C - \bar{C}_0\right)_t, \left(C - \bar{C}_0\right)_+ \right\rangle + D \int_\Omega \left|\nabla \left(C - \bar{C}_0\right)_+\right|^2 + k_B \int_{\Gamma_B} (C - C_B)\left(C - \bar{C}_0\right)_+ = \int_\Omega k_D a (C_s - C)\left(C - \bar{C}_0\right)_+,$$

or equivalently

$$\frac{1}{2}\frac{d}{dt}\left\|\left(C - \bar{C}_0\right)_+\right\|^2_{L^2(\Omega)} + D\left\|\nabla\left(C - \bar{C}_0\right)_+\right\|^2_{L^2(\Omega)} + k_B \int_{\Gamma_B} (C - C_B)\left(C - \bar{C}_0\right)_+ = \int_\Omega k_D a (C_s - C)\left(C - \bar{C}_0\right)_+.$$

Since $C_B \leq C_s \leq \bar{C}_0$, at those points where $\left(C - \bar{C}_0\right)_+ \neq 0$ we have $C - \bar{C}_0 > 0$ and then

- $C > \bar{C}_0 \geq C_B$ yields $(C - C_B)\left(C - \bar{C}_0\right)_+ \geq 0$;
- $C > \bar{C}_0 \geq C_s$ implies $(C_s - C)\left(C - \bar{C}_0\right)_+ \leq 0$.

We thereupon conclude that $\frac{1}{2}\frac{d}{dt}\left\|\left(C - \bar{C}_0\right)_+\right\|^2_{L^2(\Omega)} \leq 0$, and thus, for all $t > 0$,

$$0 \leq \left\|\left(C(t) - \bar{C}_0\right)_+\right\|_{L^2(\Omega)} \leq \left\|\left(C(0) - \bar{C}_0\right)_+\right\|_{L^2(\Omega)} = \left\|\left(C_0 - \bar{C}_0\right)_+\right\|_{L^2(\Omega)} = 0,$$

which readily implies $\bar{C}_0 - C \geq 0$ for almost every $x \in \Omega$ and $t > 0$.

In an analogous way, one can prove that $C_0 \geq C_B$ (resp. $C_0 \geq 0$) implies that $C \geq C_B$ (resp. $C \geq 0$) for almost all $t \in [0, t_F]$ and almost all $x \in \Omega$. □

Another assumption of Schauder fixed point theorem [13, Corollary 11.2] is the continuity of $T : \mathcal{G} \to \mathcal{B}$. Given $\tilde{C}_1, \tilde{C}_2 \in \mathcal{B}$, let a_1, a_2 be defined by (3.4) with $\tilde{C}_1, \tilde{C}_2$, instead of $\tilde{C}$, respectively, and let $C_1 = T(\tilde{C}_1)$, $C_2 = T(\tilde{C}_2)$. Then the difference $\delta C := C_1 - C_2$ is the weak solution to the diffusion problem

$$\begin{aligned}
\frac{\partial \delta C}{\partial t} - D\Delta \delta C &= k_D(a_1(C_s - C_1) - a_2(C_s - C_2)), && \text{in } \Omega \times (0, t_F),\\
\delta C &= 0, && \text{in } \Omega \times \{0\},\\
D\frac{\partial \delta C}{\partial \mathbf{n}} &= 0, && \text{on } \Gamma_N \times (0, t_F),\\
D\frac{\partial \delta C}{\partial \mathbf{n}} &= -k_B \delta C, && \text{on } \Gamma_B \times (0, t_F).
\end{aligned}$$

Standard energy estimates for parabolic problems yield

$$\|C_1 - C_2\|^2_{L^2(0,t_F;H^1(\Omega))} \leq \mathbb{C}_4\left(\|\tilde{C}_1 - \tilde{C}_2\|^2_{L^2(0,t_F;L^2(\Omega))} + \|a_1 - a_2\|^2_{L^\infty(0,t_F;L^2(\Omega))}\right),$$

with $\mathbb{C}_4$ depending on the problem parameters. We finally observe that, since the mapping $x \to (x)_+ := \max\{0, x\}$ is Lipschitz continuous with constant one, we have

$$\|a_1 - a_2\|^2_{L^\infty(0,t_F;L^2(\Omega))} \leq \bar{A}_0 t_F |\Omega| \|\beta\|^2_{L^\infty(\Omega)} \|\tilde{C}_1 - \tilde{C}_2\|^2_{L^2(0,t_F;L^2(\Omega))},$$

so that there exists $\mathbb{C}_5$ depending on the problem parameters such that

$$\|C_1 - C_2\|^2_{L^2(0,t_F;H^1(\Omega))} \leq \mathbb{C}_5 \|\tilde{C}_1 - \tilde{C}_2\|^2_{L^2(0,t_F;L^2(\Omega))}.$$

We thus conclude that the mapping $T : \mathcal{G} \to \mathcal{B}$ is continuous.

In order to show that all assumptions of Schauder fixed point theorem hold, we still need to prove that $T(\mathcal{G})$ is precompact in $L^2(0, t_F; L^2(\Omega))$. This is a consequence of the estimate (3.6) and Theorem 2.1 of p. 271 in [10] which implies that the space $\{v \in L^2(0, t_F; H^1(\Omega)) : v_t \in L^2(0, t_F; H^{-1}(\Omega))\}$ is compactly embedded in $L^2(0, t_F; L^2(\Omega))$. Schauder fixed point theorem [13, Corollary 11.2] thus implies the existence of a fixed point $C \in \mathcal{G}$ of T. We summarize the findings of this section in the following theorem.

Theorem 6 (*Existence*). *Let $\Omega \subset \mathbb{R}^d$ be a bounded domain with Lipschitz boundary $\partial\Omega = \Gamma_N \cup \Gamma_B$, and D, k_D, k_B and C_B positive constants, $\beta \in L^\infty(\Omega)$, $\beta \geq 0$, $0 \leq C_B \leq C_s$, and $C_0, a_0 \in L^\infty(\Omega)$, $C_0, a_0 \geq 0$. Then there exists a weak solution of (2.4), i.e., there exists a pair (C, a) of functions with $C \in L^2(0, t_F; H^1(\Omega))$, $C_t \in L^2(0, t_F; H^{-1}(\Omega))$ and $a \in H^1(0, t_F; L^2(\Omega))$ satisfying Definition 1. Furthermore, the following estimates are valid:*

$$0 \leq C \leq \bar{C}_0, \qquad 0 \leq a, \qquad \text{a.e. } (x, t) \in \Omega \times [0, t_F], \tag{3.7}$$

and, moreover, if $C_0 \geq C_B$, then $C \geq C_B$. Also,

$$a(t) = \left(\sqrt{a_0} + \frac{1}{2}\int_0^t \beta\,(C(\tau) - C_s)\,\mathrm{d}\tau\right)^2_+, \qquad \text{a.e. } (x, t) \in \Omega \times [0, t_F], \tag{3.8}$$

so that

$$0 \leq a \leq \left(\|a_0\|^{1/2}_{L^\infty(\Omega)} + \frac{1}{2} t_F \|\beta\|_{L^\infty(\Omega)} \bar{C}_0\right)^2 =: \bar{A}_0. \tag{3.9}$$

Moreover, since $\{v \in L^2(0, t_F; H^1(\Omega)) : v_t \in L^2(0, t_F; H^{-1}(\Omega))\}$ is immersed into $C([0, t_F]; L^2(\Omega))$ [10, p. 260, Lemma 1.2], C is continuous from $[0, t_F]$ into $L^2(\Omega)$.

4. Uniqueness

In this section we will study the uniqueness of weak solutions of problem (2.4). We will consider two situations that only differ in an assumption on C_0 related to the concentration of maximum solubility C_s (or saturation). We first show a situation with $C_0 > C_s$ in some region of Ω where there could exist at least two solutions. Then we will show that if $C_0 \leq C_s$ in Ω uniqueness holds.

4.1. Initial concentration above saturation

In this section we show that if $C_0 > C_s$ in some region of the domain Ω_0 of positive measure and $a_0 \equiv 0$ in Ω, then there exist at least two solutions of problem (2.4).

On the one hand, Theorem 6 guarantees the existence of a solution (C_1, a_1) of (2.4) such that $C_1 \in C([0, t_F]; L^2(\Omega))$ and

$$a_1(x, t) = \left(\frac{1}{2}\int_0^t \beta\,(C_1 - C_s)\,\mathrm{d}\tau\right)^2_+, \quad x \in \Omega,\ 0 \leq t \leq t_F.$$

We claim that $\|a_1\|_{L^2(0,t_F;L^2(\Omega))} > 0$. In fact, due to the continuity of C_1 from $[0, t_F]$ into $L^2(\Omega)$,

$$\lim_{t\to 0} \frac{1}{t}\int_{\Omega_0}\int_0^t (C_1 - C_s)\,\mathrm{d}\tau\,\mathrm{d}x = \int_{\Omega_0} (C_0 - C_s)\,\mathrm{d}x > 0.$$

Therefore, there exists $t_1 > 0$ such that

$$\int_{\Omega_0}\int_0^t (C_1 - C_s)\,\mathrm{d}\tau\,\mathrm{d}x > 0, \quad \forall t \in [0, t_1],$$

and thus $\|a_1\|_{L^2(0,t_F;L^2(\Omega))} > 0$.

On the other hand, we define $a_2 \equiv 0$ and let C_2 be the weak solution of the following classical initial/boundary problem obtained taking $a \equiv 0$ in (2.4):

$$\begin{aligned} C_t - D\Delta C &= 0, && \text{in } \Omega \times (0, t_F), \\ C &= C_0 && \text{in } \Omega \times \{0\}, \\ D\nabla C \cdot \mathbf{n} &= 0 && \text{on } \Gamma_N \times (0, t_F), \\ D\nabla C \cdot \mathbf{n} &= k_B(C_B - C) && \text{on } \Gamma_B \times (0, t_F). \end{aligned} \tag{4.1}$$

Then (C_2, a_2) is also a solution of (2.4), which is clearly different from (C_1, a_1), because $a_2 \equiv 0$ and $\|a_1\|_{L^2(0,t_f;L^2(\Omega))} > 0$.

Remark 7. In order to have more than one solution, it is necessary that $C_0 > C_s$ in some region of the domain. In the next subsection we consider the case $C_0 \leq C_s$, and we show uniqueness of solution, regardless of the initial condition for a; with the only assumption $a_0 \geq 0$. If $C_0 \leq C_s$ and $a_0 \equiv 0$, the problem (2.4) has a unique solution and it is the pair conformed by $a \equiv 0$ and C the unique solution of (4.1).

We conjecture that there could be multiple solutions when $C_0 > C_s$ in a subset of positive Lebesgue measure even if $a_0 > 0$ almost everywhere in Ω. We believe that the following situation is feasible: If a_0 is small where $C_0 < C_s$, then a will decrease and could attain zero value in finite time in that region. At the same time, by diffusion, the concentration C could grow up in that region. Then, it could happen that at a certain time $t > 0$ there will be a region of positive measure contained in Ω, where $a(\cdot, t) = 0$ and $C(\cdot, t) > C_s$. From this point on there could be two solutions like the ones presented above.

This appearance of multiple solutions is related to the high instability present in the initial phase of crystal formation.

4.2. Initial concentration below saturation

Theorem 8 (*Uniqueness*). *If $C_0 \leq C_s$ problem (2.4) has a unique solution.*

Proof. Let (C_1, a_1) and (C_2, a_2) be solutions of (2.4). Then

$$\begin{aligned}\int_\Omega (a_1 - a_2)_t w &= \int_\Omega \beta((C_1 - C_s)\sqrt{a_1} - (C_2 - C_s)\sqrt{a_2})w \\ &= \int_\Omega \beta(C_1 - C_2)\sqrt{a_1}w + \int_\Omega \beta(C_s - C_2)(\sqrt{a_2} - \sqrt{a_1})w,\end{aligned}$$

for all $w \in L^2(\Omega)$ and almost all $t \in [0, t_F]$. Taking $w = a_1 - a_2$ we obtain:

$$\frac{1}{2}\frac{d}{dt}\|a_1 - a_2\|^2_{L^2(\Omega)} = \int_\Omega \beta\sqrt{a_1}(C_1 - C_2)(a_1 - a_2) + \int_\Omega \beta(C_s - C_2)(\sqrt{a_2} - \sqrt{a_1})(a_1 - a_2). \tag{4.2}$$

From the assumption, $\bar{C}_0 = \max\{\|C_0\|_{L^\infty(\Omega)}, C_s\} = C_s$, so that by Proposition 5, $0 \leq C_1, C_2 \leq C_s$ a.e., and $C_s - C_2 \geq 0$. Also, as a consequence of the second equation in (2.7), $0 \leq a_1 \leq \|a_0\|_{L^\infty(\Omega)}$. Due to the monotonicity of the square root, $(\sqrt{a_2} - \sqrt{a_1})(a_1 - a_2) \leq 0$, so the second term of (4.2) is less than or equal to zero. Hence

$$\frac{d}{dt}\|a_1 - a_2\|^2_{L^2(\Omega)} \leq \int_\Omega (C_1 - C_2)^2 + \underbrace{\|a_0\|_{L^\infty(\Omega)}\|\beta\|^2_{L^\infty(\Omega)}}_{\mathbb{C}} \int_\Omega (a_1 - a_2)^2. \tag{4.3}$$

Analogously,

$$\langle (C_1 - C_2)_t, v\rangle + \mathscr{B}[C_1 - C_2, v] = k_D \int_\Omega (C_s - C_2)(a_1 - a_2)v - k_D \int_\Omega (C_1 - C_2)a_1 v.$$

Taking $v = C_1 - C_2$ and applying [10, Lemma 1.2, Chapter 3, p. 260] we obtain:

$$\frac{d}{dt}\|C_1 - C_2\|^2_{L^2(\Omega)} \leq 2k_D \int_\Omega (C_s - C_2)(a_1 - a_2)(C_1 - C_2) \leq k_D^2 C_s^2 \int (C_1 - C_2)^2 + \int (a_1 - a_2)^2,$$

because $0 \leq C_2 \leq C_s$ implies $0 \leq C_s - C_2 \leq C_s$. This bound and (4.3) yield

$$\frac{d}{dt}\left[\|a_1 - a_2\|^2_{L^2(\Omega)} + \|C_1 - C_2\|^2_{L^2(\Omega)}\right] \leq \max\left\{1 + k_D^2 C_s^2, 1 + \mathbb{C}\right\}\left[\|a_1 - a_2\|^2_{L^2(\Omega)} + \|C_1 - C_2\|^2_{L^2(\Omega)}\right],$$

and the claim follows by Gronwall inequality. □

5. Regularity

In this section we present regularity results for the solution (C, a) of problem (2.4) under the hypotheses that guarantee unique solution. From now on we assume that the assumptions of Theorems 6 and 8 hold and (C, a) denotes the unique weak solution of (2.4), i.e., $0 \leq C \leq C_s$, $0 \leq a \leq \|a_0\|_{L^\infty(\Omega)}$ and (3.2) holds. In each of the statements that follow, we only mention the additional assumptions that imply further regularity.

Proposition 9. *The time derivative of $\sqrt{a}$ exists and satisfies*

$$(\sqrt{a})_t = -\frac{\beta}{2}(C_s - C)\chi_{\{\sqrt{a}>0\}} \in L^2(0, t_F; L^2(\Omega)),$$

that is, $\sqrt{a} \in H^1(0, t_F; L^2(\Omega))$; also $(\sqrt{a})_t \in L^\infty(0, t_F; L^\infty(\Omega))$.

Proof. From (3.2) we have that $\sqrt{a} = \left(\sqrt{a_0} - \frac{1}{2}\int_0^t \beta(C_s - C)\,\mathrm{d}\tau\right)_+$. Since $C \in L^2(0, t_F; H^1(\Omega))$,

$$\frac{\partial}{\partial t}\sqrt{a} = -\frac{1}{2}\beta(C_s - C)\chi_{\left\{\sqrt{a_0} - \frac{1}{2}\int_0^t \beta(C_s - C)\,\mathrm{d}\tau > 0\right\}} = -\frac{1}{2}\beta(C_s - C)\chi_{\{\sqrt{a}>0\}},$$

in the weak sense in $\Omega \times (0, t_F)$, which in turn implies that $\sqrt{a} \in H^1(0, t_F; L^2(\Omega))$ and $(\sqrt{a})_t = -\frac{\beta}{2}(C_s - C)\chi_{\{\sqrt{a}>0\}}$. Besides, for a fixed t

$$\|(\sqrt{a})_t\|_{L^\infty(\Omega)} \le \frac{1}{2}\|\beta\|_{L^\infty(\Omega)}\|(C_s - C)\|_{L^\infty(\Omega)} \le \frac{1}{2}C_s\|\beta\|_{L^\infty(\Omega)},$$

due to Theorem 6, whence $(\sqrt{a})_t \in L^\infty(0, t_F; L^\infty(\Omega))$. □

In the next proposition we prove that the spatial regularity of a and $\sqrt{a}$ is higher if $\sqrt{a_0}$ and β are also more regular. It is worth mentioning though, that since there are no space derivatives in the equation for a, there is no regularizing effect. On the other hand, the appearance of $\sqrt{a}$ on the right-hand side of the equation for a_t is responsible of two issues: The value of a reaches zero at finite time, and the space regularity of $\sqrt{a}$ (resp. a) cannot be higher than $H^1(\Omega)$ (resp. $H^2(\Omega)$) after that time instant.

Proposition 10. *If $\sqrt{a_0}, \beta \in L^\infty(\Omega) \cap H^1(\Omega)$, then $\sqrt{a},\ a \in L^2(0, t_F; H^1(\Omega))$.*

Proof. From the assumption on β and the fact that $C \in L^2(0, t_F; H^1(\Omega)) \cap L^2(0, t_F; L^\infty(\Omega))$, we have $\beta\,(C_s - C) \in L^2(0, t_F; H^1(\Omega))$, and $\int_0^t \beta(C_s - C) \in L^\infty(0, t_F; H^1(\Omega))$, with $\frac{\partial}{\partial x_i}\int_0^t \beta(C_s - C) = \int_0^t \frac{\partial}{\partial x_i}(\beta(C_s - C))$. Thus, for a fixed $t \in [0, t_F]$, due to (3.2)

$$\frac{\partial}{\partial x_i}\sqrt{a} = \left(\frac{\partial}{\partial x_i}\sqrt{a_0} - \frac{1}{2}\int_0^t \frac{\partial}{\partial x_i}(\beta(C_s - C)(\tau))\,\mathrm{d}\tau\right)\chi_{\{\sqrt{a}>0\}},$$

and $\sqrt{a} \in L^2(0, t_F; H^1(\Omega))$.

Since $a = (\sqrt{a})^2$ and $\sqrt{a(t)} \in L^\infty(\Omega) \cap H^1(\Omega)$, for each t, we have $\frac{\partial}{\partial x_i}a = 2\sqrt{a}\frac{\partial}{\partial x_i}\sqrt{a}$. Now, $\sqrt{a} \in L^\infty(0, t_F; L^\infty(\Omega)) \cap L^2(0, t_F; H^1(\Omega))$ yields $\frac{\partial}{\partial x_i}a \in L^2(0, t_F; L^2(\Omega))$ and thus $a \in L^2(0, t_F; H^1(\Omega))$. □

In order to prove higher regularity of C we observe that if the pair (C, a) is a weak solution of (2.4), then C is a weak solution of the diffusion equation

$$\begin{aligned}
\frac{\partial C}{\partial t} - D\Delta C &= f, && \text{in } \Omega \times (0, t_F),\\
C &= C_0, && \text{in } \Omega \times \{0\},\\
D\frac{\partial C}{\partial \mathbf{n}} &= 0, && \text{on } \Gamma_N \times (0, t_F),\\
D\frac{\partial C}{\partial \mathbf{n}} &= k_B(C_B - C), && \text{on } \Gamma_B \times (0, t_F),
\end{aligned} \tag{5.1}$$

with $f = k_D a(C_s - C) \in L^2(0, t_F; L^2(\Omega))$, so that the same proof of Theorem 5 in [14, p. 360] allows us to conclude the following theorem.

Theorem 11. *If $C_0 \in H^1(\Omega)$, then*

$$C \in L^\infty(0, t_F; H^1(\Omega)), \qquad C_t \in L^2(0, t_F; L^2(\Omega)).$$

Assuming more regularity of C_0 and compatibility with the boundary conditions we obtain higher regularity of the concentration variable C. The proof of this result is analogous to that of Theorem 5 (ii) in [14, p. 361], taking into account the different boundary conditions, and using that $f_t = (k_D a(C_s - C))_t \in L^2(0, t_F; L^2(\Omega))$.

Theorem 12. *Let $C_0 \in H^2(\Omega)$, $D\frac{\partial C_0}{\partial \mathbf{n}} = 0$ on Γ_N, $D\frac{\partial C_0}{\partial \mathbf{n}} = k_B(C_B - C_0)$ on Γ_B, then $C_t \in L^\infty(0, t_F; L^2(\Omega)) \cap L^2(0, t_F; H^1(\Omega))$ and $C_{tt} \in L^2(0, t_F; H^{-1}(\Omega))$.*

If we assume further regularity of $\partial\Omega$ and that Γ_N and Γ_B are *separated* we can prove more space regularity for C.

Theorem 13. *Assume $C_0 \in H^2(\Omega)$, and $D\frac{\partial}{\partial \mathbf{n}}C_0 = 0$ on Γ_N, $D\frac{\partial}{\partial \mathbf{n}}C_0 = k_B(C_B - C_0)$ on Γ_B. If $\Omega \subset \mathbb{R}^d$ has a boundary $\Gamma \in C^{1,1}$ such that $\Gamma = \Gamma_N \cup \Gamma_B$ and $\mathrm{dist}\{\Gamma_N,\ \Gamma_B\} > 0$, then $C \in L^\infty(0, t_F; H^2(\Omega))$.*

Remark 14. The assumption $\operatorname{dist}\{\Gamma_N,\ \Gamma_B\} > 0$ is only necessary for the existence of $\theta \in C^\infty(\mathbb{R}^d)$ such that $\theta\,|_{\Gamma_N} = 0$ and $\theta\,|_{\Gamma_B} = 1$. This will allow for an extension of the boundary values which will in turn permit the use of elliptic regularity to conclude the assertion of the theorem. Many commercial devices have their outer boundary releasing drug to the bulk medium, whereas they have an inner boundary touching a solid elastic core, which is insulating; this assumption is thus fulfilled in practical applications.

Proof. By Theorem 11 we know that $C \in L^\infty(0, t_F; H^1(\Omega))$, $C_t \in L^2(0, t_F; L^2(\Omega))$ and

$$\langle C_t, v\rangle + \mathscr{B}[C, v] + k_D \int_\Omega aCv = k_D \int_\Omega aC_s v + k_B C_B \int_{\Gamma_B} v, \quad \forall v \in H^1,\ \text{a.e. } t \in (0, t_F),$$
$$C(0) = C_0.$$

Let us define $f := k_D C_s a - C_t - k_D aC$. Theorem 11 implies that $f(t) \in L^2(\Omega)$ for almost every $t \in [0, t_F]$, for which $C(t)$ is a weak solution of the following (elliptic) problem:

$$\begin{aligned} -D\Delta C &= f, && \text{in } \Omega \\ D\frac{\partial C}{\partial \mathbf{n}} &= 0, && \text{on } \Gamma_N, \\ D\frac{\partial C}{\partial \mathbf{n}} &= -k_B(C - C_B), && \text{on } \Gamma_B. \end{aligned}$$

Since $\operatorname{dist}\{\Gamma_N,\ \Gamma_B\} > 0$, there exists $\theta \in C^\infty(\mathbb{R}^d)$ such that $\theta|_{\Gamma_N} = 0$ and $\theta|_{\Gamma_B} = 1$. Let us define $g := -k_B(C - C_B)\theta$. Then $g(t) \in H^1(\Omega)$ for almost every $t \in [0, t_F]$ because $C(t) \in L^\infty(\Omega) \cap H^1(\Omega)$ for almost every $t \in [0, t_F]$ and $\theta \in C^\infty(\mathbb{R}^d)$.

Moreover, for almost all $t \in [0, t_F]$, $\|g\|_{H^1(\Omega)} \le \mathbb{C}\|C\|_{H^1(\Omega)} + \tilde{\mathbb{C}}$ where $\mathbb{C}$, $\tilde{\mathbb{C}}$ depend on θ, C_B and k_B. By construction, $g|_{\Gamma_B} = -k_B(C - C_B)$ and $g|_{\Gamma_N} = 0$, and then $C(t)$ is weak solution of

$$\begin{aligned} -D\Delta C + C &= \tilde{f} := f + C, && \text{in } \Omega \\ D\frac{\partial C}{\partial \mathbf{n}} &= g, && \text{on } \partial\Omega. \end{aligned}$$

Finally by Corollary 2.2.2.6 [15, p. 92], we have that $C \in H^2(\Omega)$ and

$$\|C\|_{H^2(\Omega)} \le \tilde{\tilde{\mathbb{C}}}\left(\|f + C\|_{L^2(\Omega)} + \|g\|_{H^1(\Omega)}\right) \le \mathbb{C}\left(\|f\|_{L^2(\Omega)} + \|C\|_{L^2(\Omega)} + \mathbb{C}_1\|C\|_{H^1(\Omega)} + \tilde{\mathbb{C}}\right),$$

where $\tilde{\tilde{\mathbb{C}}}$ depend on Ω and D. By Theorems 12 and 11, we have $\|C\|_{L^\infty(0,t_F;H^2(\Omega))}$ is finite. □

It is interesting to note that regularity results for this problem have a limitation due to the presence of $\sqrt{a}$. This term implies that a vanishes in positive measure sets at finite time, and $a(t)$ does not belong to $H^3(\Omega)$ even if a_0 belongs to $H^\infty(\Omega)$.

6. Discretization and simulations

In this section we present a finite element discretization and some simulations which show an excellent agreement with laboratory experiments. Besides, they allow us to visualize some features of the evolution, such as the lack of regularizing effect on the variable a. The proof of the error estimates is postponed to Section 7.

6.1. Finite element discretization and error estimates

We consider a conforming and shape regular triangulation $\mathcal{T} = \mathcal{T}_h$ of Ω, such that $\cup_{T\in\mathcal{T}_h} T = \bar{\Omega}$ with $h := \max_{T\in\mathcal{T}_h} \operatorname{diam}(T)$, and the following finite element spaces:

$$V_h = \{v \in H^1(\Omega) : v|_T \in \mathscr{P}_1,\ \forall T \in \mathcal{T}_h\}, \qquad W_h = \{w \in L^2(\Omega) : w|_T \in \mathscr{P}_0,\ \forall T \in \mathcal{T}_h\},$$

where $\mathscr{P}_\ell$ is the space of polynomials of degree less than or equal to ℓ.

Let Δt be the time step, and let $t_n = n\Delta t,\ n = 0, 1, \ldots$. Using a backward Euler discretization for C and taking into account formula (3.2) for a we arrive at the following definition of C^n and a^n, which denote the approximations of $C(t_n)$ and $a(t_n)$, respectively. Let $C^n \in V_h$ and $a^n \in W_h$ be defined as:

$$\begin{aligned} (C^n, v) + \Delta t\mathscr{B}[C^n, v] + \Delta t k_D(C^n a^{n-1}, v) &= \Delta t k_D C_s(a^{n-1}, v) + \Delta t k_B(C_B, v)_{\Gamma_B} + (C^{n-1}, v), \quad \forall v \in V_h, \\ \sqrt{a^n} &= \left(\sqrt{a^{n-1}} - \frac{1}{2}\int_{t_{n-1}}^{t_n} \bar{\beta}(C_s - \bar{C}^n)_+\right)_+, \end{aligned} \tag{6.1}$$

for $n = 1, 2, \ldots$, with $\bar{C}^n$ the $L^2(\Omega)$-projection of C^n on W_h; $C^0 \in V_h$ and $a^0 \in W_h$ the initial discrete conditions and $(\cdot, \cdot)$ denotes the $L^2(\Omega)$ product. We chose C^0 as the Lagrange interpolant of C_0 and a^0 as the $L^2(\Omega)$-projection of a_0 on W_h.

Table 1
Initial conditions and parameter values for the CIDR device.

C_0	0.513 (kg/m^3)
$m_{0,p}$	1.0550e−12 (kg)
$a_{0,p}$	4.5239e−10 (m^2)
D_{ap40}	1.670e−10 (m^2/s)
D_{ap60}	2.701e−10 (m^2/s)
Num	1 791 672 552
k_D	6.59e−6 (m/s)
k_B	1e−3 (m/s)
C_s	0.513 (kg/m^3)
V	1.9075e−5 (m^3)
ρ_s	1.1660285e+03 (kg/m^3)
C_B	0

Existence of $\{(C^n, a^n)\}_{n\geq 1}$, stability bounds and the following error estimates are proven in Section 7. From now on (C, a) denotes the weak solution to (2.4) and $\{(C^n, a^n)\}_{n\geq 1}$ are given by (6.1).

Theorem 15. *If $a \in H^1(0, t_F; L^2(\Omega))$, $C \in H^1(0, t_F; H^1(\Omega))$ and $C_{tt} \in L^2(0, t_F; H^{-1}(\Omega))$, then*

$$\max_{1\leq n\leq t_F/\Delta t} \left\|C^n - C(t_n)\right\|_{L^2(\Omega)} + \left\|\sqrt{a^n} - \sqrt{a(t_n)}\right\|_{L^2(\Omega)} \leq \mathbb{C}^*_{t_F}\left[\left\|C^0 - C(0)\right\|_{L^2(\Omega)} + \left\|\sqrt{a^0} - \sqrt{a(0)}\right\|_{L^2(\Omega)} + h + \Delta t\right],$$

where $\mathbb{C}^*_{t_F}$ depends on $\|a\|_{H^1(0,t_F;L^2(\Omega))}$, $\|C\|_{H^1(0,t_F;H^1(\Omega))}$ and $\|C_{tt}\|_{L^2(0,t_F;H^{-1}(\Omega))}$ and the parameters of the problem, but is independent of the discretization parameters h and Δt.

Using the regularity estimates from Section 5 we obtain the following corollary.

Corollary 16. *If $C_0 \in H^2(\Omega)$, $D\frac{\partial}{\partial \mathbf{n}}C_0 = 0$ on Γ_N, $D\frac{\partial}{\partial \mathbf{n}}C_0 = k_B(C_B - C_0)$ on Γ_B then the assertion of Theorem 15 holds with $\mathbb{C}^*_{t_F}$ depending on the end time t_F, on $\|a_0\|_{L^\infty(\Omega)}$, $\|C_0\|_{H^2(\Omega)}$ and on the parameters k_D, C_s, $\|\beta\|_{L^\infty(\Omega)}$ of the problem, listed in (2.5), but independent of h and Δt.*

Furthermore, if we assume that the assumptions of Theorem 13 hold, then $C \in L^\infty(0, t_F; H^2(\Omega))$ and we find a bound for the error of C in a discrete norm analogous to the $L^2(0, t_F; H^1(\Omega))$-norm.

Theorem 17. *Assume that Ω has boundary of class $C^{1,1}$ and $\operatorname{dist}\{\Gamma_N, \Gamma_B\} \neq 0$. If $C_0 \in H^2(\Omega)$ and $D\frac{\partial}{\partial \mathbf{n}}C_0 = 0$ on Γ_N and $D\frac{\partial}{\partial \mathbf{n}}C_0 = k_B(C_B - C_0)$ on Γ_B. Then there exists a constant $\tilde{\mathbb{C}}^*_{t_F}$ that depends on the final time t_F, on $\|a_0\|_{L^\infty(\Omega)}$, $\|C_0\|_{H^2(\Omega)}$ and on the parameters k_D, C_s, $\|\beta\|_{L^\infty(\Omega)}$ of the problem, listed in (2.5), but is independent of h and Δt, and*

$$\left(\sum_{j=1}^{\lceil t_F/\Delta t\rceil} \Delta t\|C^j - C(t_j)\|^2_{H^1(\Omega)}\right)^{1/2} \leq \tilde{\mathbb{C}}^*_{t_F}\left[\|C^0 - C(0)\|_{H^1(\Omega)} + \|\sqrt{a^0} - \sqrt{a(0)}\|_{L^2(\Omega)} + h + \Delta t\right].$$

6.2. Simulations

We now report some qualitative and quantitative properties of the solutions of (2.4), which we obtained from computing with the numerical method presented in the previous section. The code was developed in MATLAB using ideas from [16,17] for the fast assembling of the linear systems.

We focus on the solution of the problem on the commercial device called CIDR (InterAg Manufacturing, New Zealand) and alluded to in the Introduction (see Fig. 1). We recall that it is initially loaded with 1.9 g of Progesterone, and is used by cattle producers to achieve estrous synchronization, which in turn allow a better outcome of artificial insemination; see [18] and references therein.

The parameter values used for the simulation of the drug release from this device, taken from [18], are stated in Table 1; C_0 denotes the initial concentration of dissolved drug and $m_{0,p}$, $a_{0,p}$ stand for the initial mass and area of each particle of solid drug, respectively, whereas Num is the total number of particles in the device, which we assumed evenly distributed. The diffusion coefficients D_{ap40} and D_{ap60} correspond to a liberation media with 40% and 60% ethanol in water, respectively, and k_D is the dissolution rate of the particles of solid drug. The coefficient k_B is a mass transference coefficient and C_s is the saturation concentration or maximum solubility. V denotes the volume of the device, ρ_s the intrinsic density of the solid drug particles and C_B the concentration of drug in the liberation medium.

Even though the device is three-dimensional, we assumed that it is composed of two cylindrical pieces, insulated at both ends. One piece is 19 cm long with cross section A–A′as in Fig. 1 (right), and another one is 10.37 cm long with cross section B–B′. The lengths have been chosen to match the volume of the original device. This simplification allows us to compute on two-dimensional domains, saving a lot of computational time; the comparison of drug release with laboratory experiments is excellent, so this dimension reduction is worthwhile.

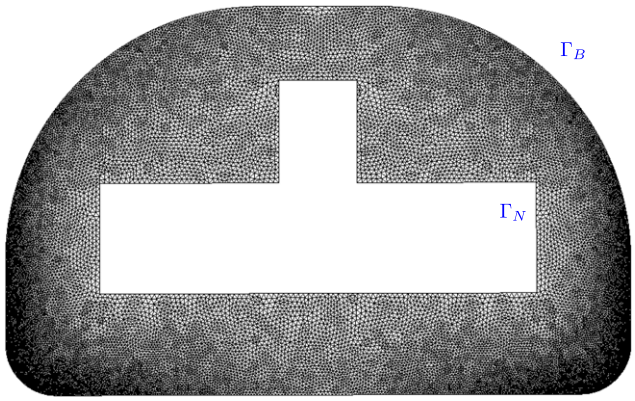

Fig. 2. Triangulation of 22 847 vertices and 44 392 elements, for the cross section A–A′of the CIDR device.

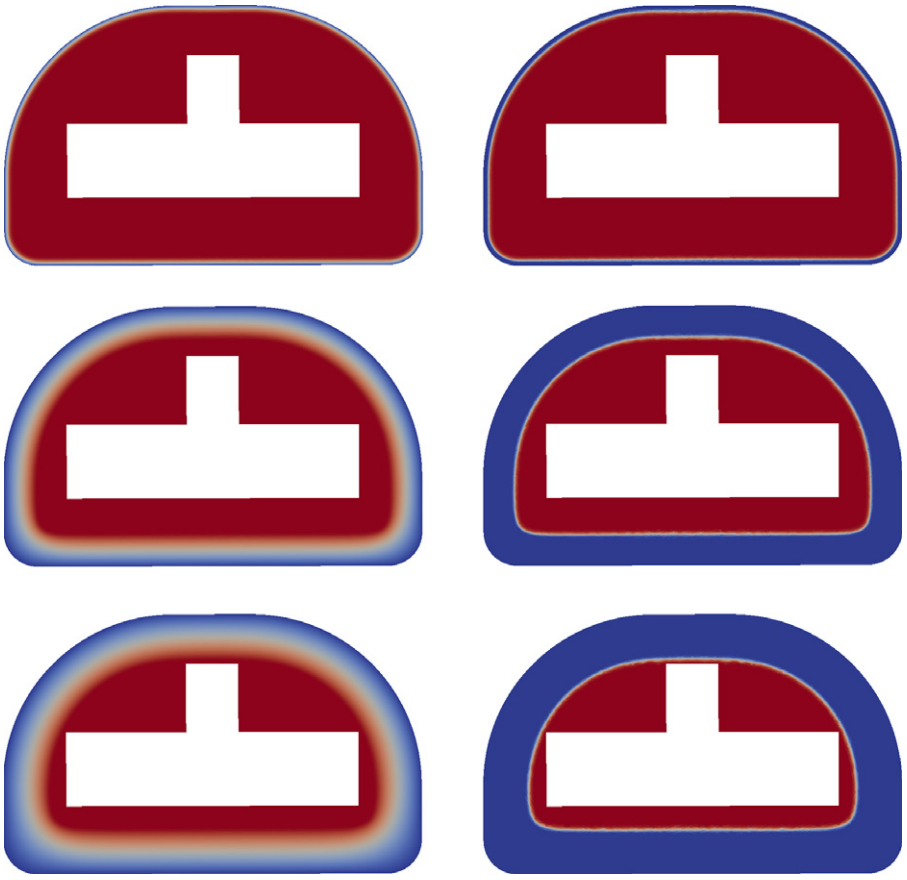

Fig. 3. Concentration of dissolved drug C (left) and area per unit volume of solid drug particles a (right) at $t = 3hs$ (top), $84hs$ (middle) and $168hs$ (bottom).

6.3. Transversal section A–A′

In order to compute on the cylindrical piece with transversal section A–A′, we generated a mesh with Gmsh version 2.5.1 [19] for the A–A′section and $h = 0.22 \times 10^{-7}$ m, which has 22 847 vertices and 44 392 elements; see Fig. 2.

In Fig. 3 we show the distribution, at different time instants, of dissolved drug C and area per unit volume of the solid drug particles a.

We can observe that C is smoother than a, due to the regularizing effect of the term $D\Delta C$ in the differential equation. It can also be observed that there is a front separating the region where $a = 0$ from the region where $a > 0$. The function C is smoother and satisfies a diffusion equation in the region where a vanishes, with a Robin-type boundary condition in the outer boundary of the device and Dirichlet-type boundary condition $C = C_s$ at the interface where a starts to be positive.

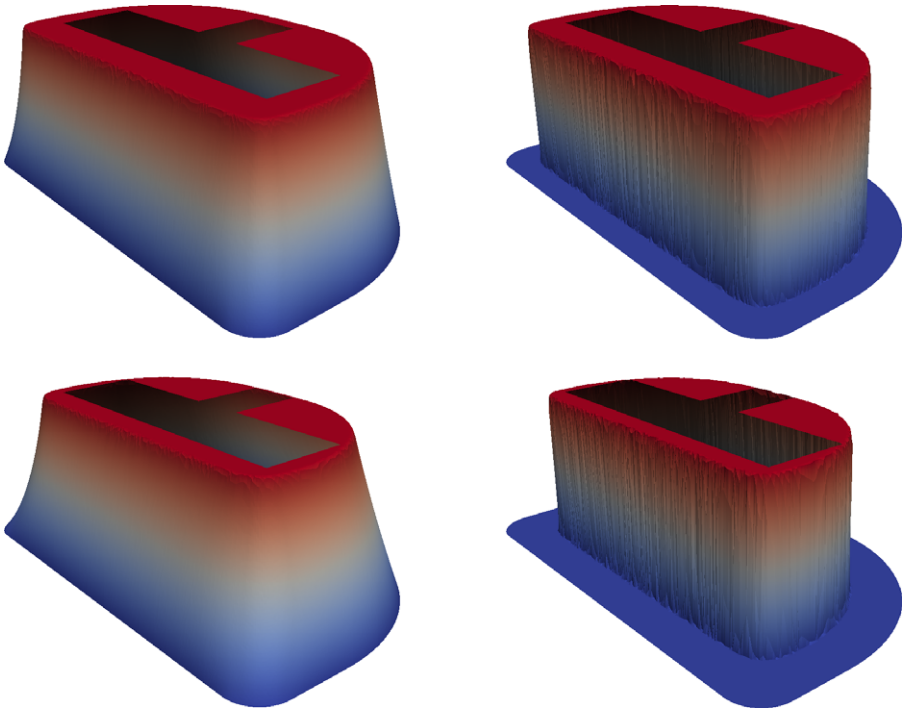

Fig. 4. Three-dimensional profile of the dissolved drug concentration C (left) and the area of solid particles per unit volume a (right) for $t = 84hs$ (top) and $t = 168hs$ (bottom). We see that $C \approx C_s$ where $a > 0$ and C looks like a solution to a pure diffusion equation where $a = 0$, with a Robin-type boundary condition in the outer boundary.

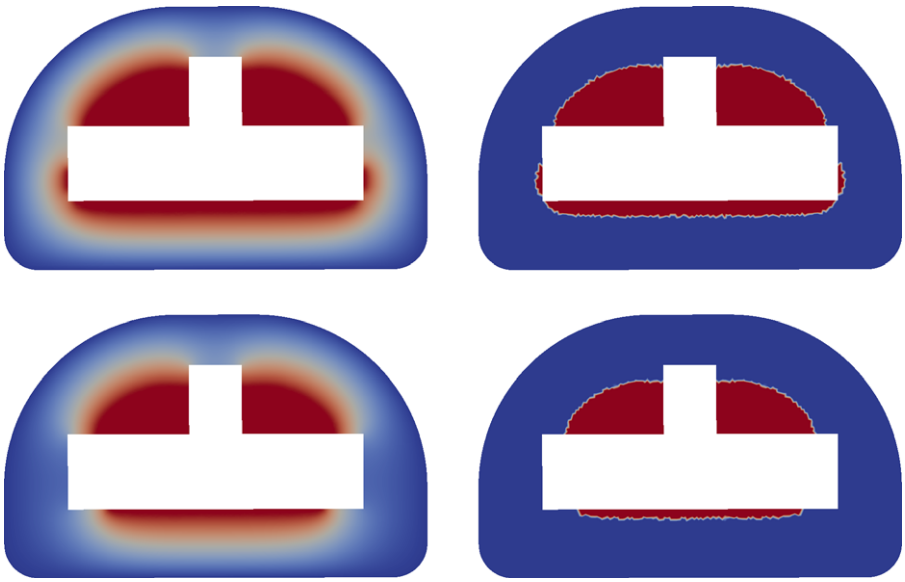

Fig. 5. Concentration of dissolved drug C (left) and area per unit volume of solid drug particles a (right) at $t = 276hs$ (top) and $t = 336hs$ (bottom).

In order to observe better these features we plot a 3D-graphic of C and a in Fig. 4 for $t = 84hs$ and $t = 168hs$. We see that $C \approx C_s$ where $a > 0$ and C looks like a solution to a pure diffusion equation where $a = 0$. It is also worth observing the lack of regularity of a, in contrast to the regularity of C, which is enforced by the diffusion term $D\Delta C$.

We end this section showing in Fig. 5 the concentration of dissolved drug C and the area of the solid drug particles for times t greater than seven days. Even though these devices are used for a one-week period, it is important to know how much drug remains inside the device, and where, in order to optimize their shape to minimize negative consequences to the environment.

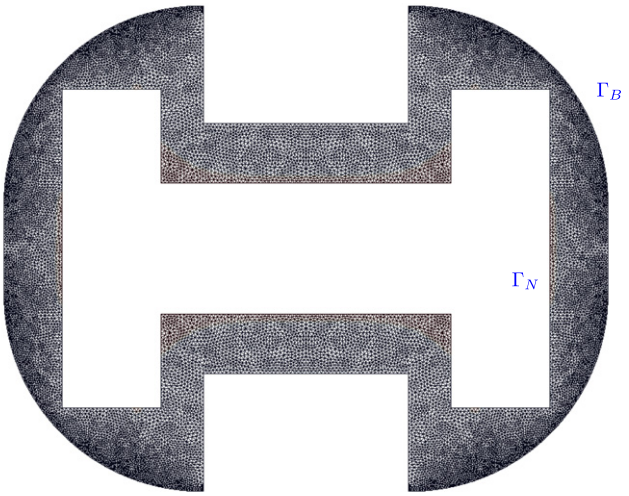

Fig. 6. Triangulation of 16 184 vertices and 30 888 elements, for the cross section B–B′of the CIDR device.

6.4. Transversal section B–B′

Computation of the solution

To compute on the cylindrical piece with transversal section B–B′as in Fig. 1 (right), we generated a mesh of the B–B′section with Gmsh, obtaining a triangulation with $h = 1.32 \times 10^{-7}$ m, 16 184 vertices and 30 888 elements (see Fig. 6).

In Fig. 7 we show the distribution of dissolved drug and area per unit volume of the solid drug particles, for different time instants.

6.5. Comparison with experimental data

We now compare our numerical results with experimental data obtained at Instituto de Desarrollo Tecnológico para la Industria Química (INTEC–CONICET–UNL). They performed measurements of released drug from CIDR devices *in vitro*. Several devices were sunk into different stirred containers with 40% and 60% of ethanol in water. The released drug from the devices was measured after 1, 2, 3, 4, 5, 6, 12, 24 h, and from that moment on, once every 24 h, for seven days.

We computed the total amount of released drug at time t from each piece using the following formula:

$$\begin{aligned} Q(t) &= \text{total amount of initial drug} - \text{total amount of drug at time } t \\ &= \text{Num} \times m_{0,p} - \frac{\rho_S L}{6\sqrt{\pi}} \int_\Omega \frac{a^{3/2}}{\sqrt{N}} - L \int_\Omega C, \end{aligned}$$

where L is the length of the piece and Ω is the two-dimensional cross section.

The sum of the drug released by both pieces according to our numerical calculations, versus the experimental measurements can be observed in Fig. 8.

We observe that the computations according to this proposal fit the experimental data very well. Visually, the fit is equal to the one obtained in [18], where three-dimensional computations, on a mesh with 3 816 762 elements were performed. It is interesting to note that adding the contributions of the two bi-dimensional meshes that we used, we arrive at 75 280 elements and 39 031 vertices. The computational cost of our proposal is significantly lower.

Remark 18. If we consider initial conditions $a_0 \equiv 0$ in Ω with $C_0 > C_s$ in some region, we know that there are multiple solutions (see Section 4.1). From (6.1) we notice that the numerical method will choose the solution with $a \equiv 0$, and therefore will approximate the pure diffusion problem (4.1) for the variable C measuring the concentration of dissolved drug.

7. Proofs of error estimates

The main goal of this section is to prove Theorems 15 and 17, which state error estimates for the discretization proposed in Section 6.

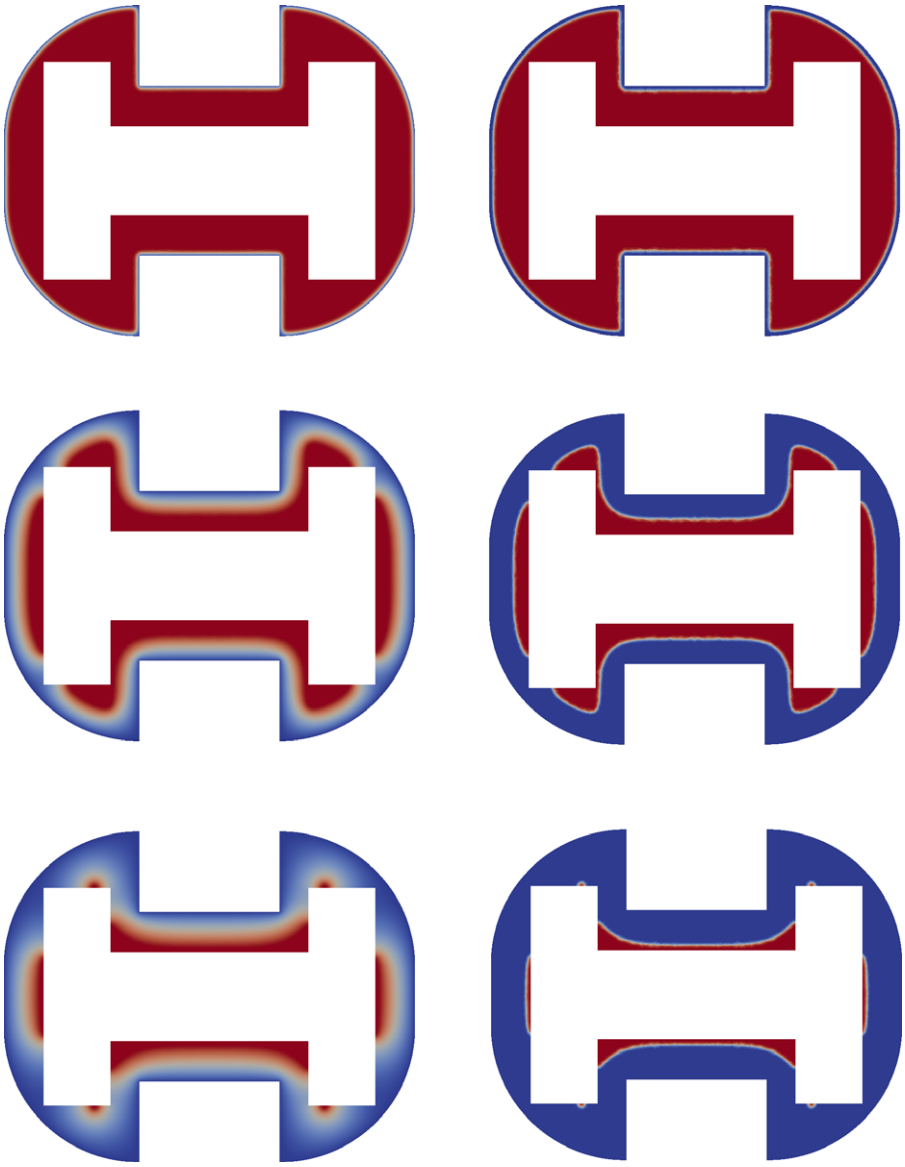

Fig. 7. Concentration of dissolved drug C (left) and area per unit volume of solid drug particles a (right) at $t = 3hs$ (top), $84hs$ (middle) and $168h$ s (bottom).

7.1. Existence

Observing (6.1) we notice that the definition of C^n involves a^{n-1} and not a^n, so that C^n can be computed first. Writing the first equation of (6.1) using a basis for V_h we are led to a linear system with a symmetric positive definite matrix, and existence of C^n is thus guaranteed. The definition of a^n in the second equation of (6.1) can be simplified as

$$\sqrt{a^n} = \left(\sqrt{a^{n-1}} - \frac{1}{2}\Delta t\bar{\beta}(C_s - \bar{C}^n)_+\right)_+,$$

where we have changed the integral in the definition of a^n by a multiplication by Δt.

In order not to clutter the notation, in the rest of the article we will use $\|\cdot\|$ to denote the $L^2(\Omega)$-norm, $\|\cdot\|_{H^1}$ to denote the $H^1(\Omega)$-norm, $\|\cdot\|_{L^2(H^1)}$ to denote the $L^2(0, t_F; H^1(\Omega))$-norm, etc.

7.2. Stability

From the definition of a^n we observe that $0 \le a^n \le a^{n-1}$, so that $\|a^n\| \le \|a^{n-1}\| \le \cdots \le \|a^0\|$.

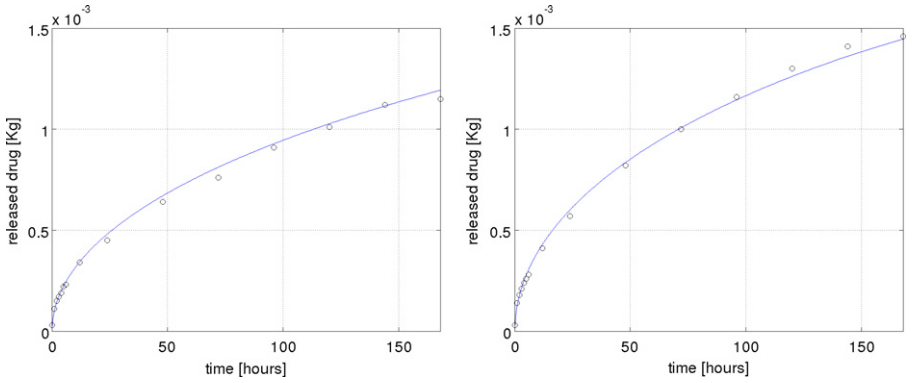

Fig. 8. Drug release according to the numerical simulation versus experimental measurements in a solution of 40% ethanol in water (left) and 60% (right). The simulation was done considering a device composed of two cylindrical pieces. One shaped as the A–A′cut and length 19 cm, the other one shaped as B–B′and length 10.37 cm. The agreement between our computations and the measurements is remarkable, and comparable to the computations on the three-dimensional domain reported in [18]; where meshes with almost four million elements were needed.

To study the stability of C^n, we take $v = C^n$ in (6.1) and obtain

$$(C^n, C^n) + \Delta t \mathscr{B}[C^n, C^n] + \Delta t k_D (C^n a^{n-1}, C^n) \leq \Delta t k_D C_s \|a^{n-1}\| \, \|C^n\| + \Delta t k_B C_B |\Gamma_B|^{1/2} \|C^n\|_{L^2(\Gamma_B)} + \|C^{n-1}\| \, \|C^n\|.$$

By the Cauchy inequality and (2.9)

$$\|C^n\|^2 + \Delta t \mathscr{B}[C^n, C^n] \leq \frac{\Delta t}{D} k_D^2 C_s^2 \|a^{n-1}\|^2 + \Delta t k_B C_B^2 |\Gamma_B| + \|C^{n-1}\|^2,$$

which yields the existence of $\mathbb{C}_6, \mathbb{C}_7, \mathbb{C}_8$ depending on problem data such that

$$\|C^n\|^2 - \|C^{n-1}\|^2 + \Delta t \mathbb{C}_1 \|C^n\|_{H^1}^2 \leq \Delta t \left(\mathbb{C}_6 \|a^{n-1}\|^2 + \mathbb{C}_7\right) \leq \mathbb{C}_8 \Delta t.$$

Adding on n from 1 to $M = \lceil t_F / \Delta t \rceil$ we obtain the following stability estimates:

$$\max_{1 \leq n \leq M} \|C^n\|^2, \ \mathbb{C}_1 \Delta t \sum_{n=1}^{M} \|C^n\|_{H^1}^2 \leq \|C^0\|^2 + \mathbb{C}_8 t_F. \tag{7.1}$$

7.3. Error estimation

In what follows we will make use of the L^2-projection on W_h and the *Ritz projection* on V_h.

As in the definition of a^n, $\bar{u}$ denotes the L^2-projection of u onto W_h, i.e., $\bar{u} \in W_h$ and $(\bar{u}, \chi_T) = (u, \chi_T)$, for all $T \in \mathcal{T}_h$. Applying the Poincaré–Friedrich inequality, using that $\bar{u}_{|T} = \frac{1}{|T|} \int_T u$ for each $T \in \mathcal{T}_h$ we obtain that

$$\|\bar{u} - u\| \leq \mathbb{C}^* h \|u\|_{H^1}, \quad \forall u \in H^1(\Omega), \tag{7.2}$$

where $\mathbb{C}^*$ is a constant that depends only on the dimension of the space.

Also, we define $R_h u$ as the *Ritz projection* with respect to the inner product induced by the bilinear form $\mathscr{B}[\cdot, \cdot]$ in $H^1(\Omega)$, i.e.,

$$R_h u \in V_h : \ \mathscr{B}[R_h u - u, v] = 0, \quad \forall v \in V_h.$$

Standard interpolation theory [20–22] and error estimates of finite elements for stationary problems allow us to affirm that, if Ω has boundary of class $C^{1,1}$ and $\operatorname{dist}(\Gamma_N, \Gamma_B) > 0$, then

$$\|R_h v - v\| \leq \tilde{\mathbb{C}} h \|v\|_{H^1}, \quad \forall v \in H^1(\Omega), \tag{7.3}$$

and

$$\|R_h v - v\|_{H^1} \leq \tilde{\mathbb{C}} h \|v\|_{H^2}, \quad \forall v \in H^2(\Omega), \tag{7.4}$$

with $\tilde{\mathbb{C}}$ depending on the mesh regularity.

Remark 19. The assumptions about the regularity of $\partial\Omega$ and the distance between boundaries of different kind guarantee that the elliptic problem has H^2 regularity, i.e., given a source term $L^2(\Omega)$ the solution belongs to $H^2(\Omega)$. Estimate (7.4) is a consequence of Céa lemma and standard interpolation estimates. The proof of (7.3) uses the *Aubin–Nitsche trick*.

The following estimates will be used in the proof of the main result. Their proof is straightforward and will thus be omitted.

Lemma 20. *Let $C \in H^1(0, t_F; H^1(\Omega))$ and $C_{tt} \in L^2(0, t_F; H^{-1}(\Omega))$ then*

$$\|\overline{\partial}_t R_h C(t_n) - \overline{\partial}_t C(t_n)\|^2 \leq \frac{\tilde{\mathbb{C}}^2 h^2}{\Delta t} \int_{t_{n-1}}^{t_n} \|C_t\|_{H^1}^2 \, \mathrm{ds}, \quad \|C_t(t_n) - \overline{\partial}_t C(t_n)\|_{H^{-1}}^2 \leq \Delta t \int_{t_{n-1}}^{t_n} \|C_{tt}(s)\|_{H^{-1}}^2 \, \mathrm{ds}.$$

Hereafter, $\overline{\partial} v(t_n) = (v(t_n) - v(t_{n-1}))/\Delta t$.

In order to prove Theorem 15 we split the error $C^n - C(t_n)$ as a sum of two terms:

$$C^n - C(t_n) = (C^n - R_h C(t_n)) + (R_h C(t_n) - C(t_n)) := \theta_C^n + \rho_C^n. \tag{7.5}$$

The term ρ_C^n is easy to bound using the spatial regularity of C and (7.3)–(7.4). The main goal of the next lemma is to bound the L^2-norm of θ_C^n.

Lemma 21. *Under the assumptions of Theorem 15, we have, for $n = 1, 2, \ldots, M$,*

$$\begin{aligned}\|\theta_C^n\|^2 \leq \|\theta_C^{n-1}\|^2 + \mathbb{C}_9 \Delta t \Big(&\|\sqrt{a^{n-1}} - \sqrt{a(t_{n-1})}\|^2 + \Delta t \int_{t_{n-1}}^{t_n} \|a_t(s)\|^2 \, \mathrm{ds} + \tilde{\mathbb{C}}^2 h^2 \|C\|_{L^\infty(H^1)}^2 \\ &+ \frac{\tilde{\mathbb{C}}^2 h^2}{\Delta t} \int_{t_{n-1}}^{t_n} \|C_t(s)\|_{H^1}^2 \, \mathrm{ds} + \Delta t \int_{t_{n-1}}^{t_n} \|C_{tt}(s)\|_{H^{-1}}^2 \, \mathrm{ds} \Big).\end{aligned} \tag{7.6}$$

Proof. If we denote $\overline{\partial}_t C^n = (C^n - C^{n-1})/\Delta t$, the first line of (6.1) reads:

$$\mathscr{B}[C^n, v] = k_D \int_\Omega (C_s - C^n) a^{n-1} v + k_B C_B \int_{\Gamma_B} v - \int_\Omega \overline{\partial}_t C^n v, \quad \forall v \in V_h.$$

On the other hand, $R_h C(t_n)$ satisfies

$$\mathscr{B}[R_h C(t_n), v] = k_D \int_\Omega (C_s - C(t_n)) a(t_n) v + k_B C_B \int_{\Gamma_B} v - \int_\Omega C_t(t_n) v,$$

for all $v \in V_h$. Subtracting the above identities, we have, for all $v \in V_h$

$$\begin{aligned}\mathscr{B}[\underbrace{C^n - R_h C(t_n)}_{\theta_C^n}, v] &= k_D \int_\Omega (C_s - C^n) a^{n-1} v - k_D \int_\Omega (C_s - C(t_n)) a(t_n) v + \int_\Omega (C_t(t_n) - \overline{\partial}_t C^n) v, \\ &= k_D \int_\Omega (C_s - C(t_n))(a^{n-1} - a(t_n)) v + k_D \int_\Omega (C(t_n) - C^n) a^{n-1} v + \int_\Omega (C_t(t_n) - \overline{\partial}_t C^n) v.\end{aligned}$$

Recalling that $\theta_C^n = C^n - R_h C(t_n)$ and setting $v = \theta_C^n \in V_h$ we are led to the following bound

$$\begin{aligned}\mathscr{B}[\theta_C^n, \theta_C^n] \leq\ & k_D \int_\Omega (C_s - C(t_n))(a^{n-1} - a(t_n)) \theta_C^n - k_D \int_\Omega \underbrace{(R_h C(t_n) - C(t_n))}_{\rho_C^n} a^{n-1} \theta_C^n \\ &+ \int_\Omega \Big(C_t(t_n) - \overline{\partial}_t C(t_n) + \underbrace{\overline{\partial}_t C(t_n) - \overline{\partial}_t R_h C(t_n)}_{-\overline{\partial}_t \rho_C^n} + \underbrace{\overline{\partial}_t R_h C(t_n) - \overline{\partial}_t C^n}_{-\overline{\partial}_t \theta_C^n} \Big) \theta_C^n.\end{aligned}$$

Therefore

$$\begin{aligned}\int_\Omega \underbrace{\overline{\partial}_t \theta_C^n \, \theta_C^n}_{\frac{1}{\Delta t}\left(\theta_C^n \theta_C^n - \theta_C^{n-1} \theta_C^n\right)} + \mathscr{B}[\theta_C^n, \theta_C^n] \leq\ & k_D \Big(C_s \|a^{n-1} - a(t_n)\| + \|a^{n-1}\|_{L^\infty} \|\rho_C^n\| + \frac{1}{k_D} \|\overline{\partial}_t \rho_C^n\| \Big) \|\theta_C^n\| \\ &+ \|C_t(t_n) - \overline{\partial}_t C(t_n)\|_{H^{-1}} \|\theta_C^n\|_{H^1}\end{aligned}$$

where we have used that $0 \leq C \leq C_s$ (cf. Theorem 6). Owing to Cauchy inequality, we obtain

$$\begin{aligned}\|\theta_C^n\|^2 + \frac{\Delta t}{2} \mathscr{B}[\theta_C^n, \theta_C^n] \leq\ & \|\theta_C^{n-1}\| \, \|\theta_C^n\| + \Delta t \mathbb{C} \Big[\Big(k_D C_s \|a^{n-1} - a(t_{n-1})\| + k_D C_s \|a(t_{n-1}) - a(t_n)\| \\ &+ k_D \|a^{n-1}\|_\infty \|\rho_C^n\| + \|\overline{\partial}_t \rho_C^n\| \Big)^2 + \|C_t(t_n) - \overline{\partial}_t C(t_n)\|_{H^{-1}}^2 \Big].\end{aligned}$$

Thus, using that $0 \le a^{n-1}, a(t_{n-1}) \le \bar{A}_0$,

$$\|\theta_C^n\|^2 + \Delta t \mathscr{B}[\theta_C^n, \theta_C^n] \le \|\theta_C^{n-1}\|^2 + 2\Delta t \mathbb{C}\Big[\Big(k_D C_s 2\sqrt{\bar{A}_0}\|\sqrt{a^{n-1}} - \sqrt{a(t_{n-1})}\| + k_D C_s \Big\| \int_{t_{n-1}}^{t_n} a_t(s)\,\mathrm{d}s \Big\| + k_D \bar{A}_0 \|\rho_C^n\| + \|\bar{\partial}_t \rho_C^n\|\Big)^2 + \|C_t(t_n) - \bar{\partial}_t C(t_n)\|^2_{H^{-1}(\Omega)}\Big].$$

Finally, taking into account the estimates of Lemma 20

$$\|\theta_C^n\|^2 + \Delta t \mathscr{B}[\theta_C^n, \theta_C^n] \le \|\theta_C^{n-1}\|^2 + \mathbb{C}_9 \Delta t \Big(\|\sqrt{a^{n-1}} - \sqrt{a(t_{n-1})}\|^2 + \Delta t \int_{t_{n-1}}^{t_n} \|a_t(s)\|^2\,\mathrm{d}s + \tilde{\mathbb{C}}^2 h^2 \|C\|^2_{L^\infty(H^1)} + \frac{\tilde{\mathbb{C}}^2 h^2}{\Delta t} \int_{t_{n-1}}^{t_n} \|C_t(s)\|^2_{H^1}\,\mathrm{d}s + \Delta t \int_{t_{n-1}}^{t_n} \|C_{tt}(s)\|^2_{H^{-1}}\,\mathrm{d}s \Big). \tag{7.7}$$

The claim follows by dropping the term $\Delta t \mathscr{B}[\theta_C^n, \theta_C^n]$ from the left-hand side. □

Lemma 22. *Under the assumptions of Theorem 15, we have, for $n = 1, 2, \ldots, M$,*

$$\Big\|\sqrt{a^n} - \sqrt{a(t_n)}\Big\| \le \Big\|\sqrt{a^{n-1}} - \sqrt{a(t_{n-1})}\Big\| + \Delta t \mathbb{C}_{10}\big(\|\theta_C^n\| + h\|C^n\|_{H^1} + h\|C(t_n)\|_{H^1} + \Delta t \|C_t\|_{L^\infty(L^2)} + h\big), \tag{7.8}$$

where $\mathbb{C}_{10}$ is a constant depending on C_s, β and $\mathbb{C}^*$.

Proof. Recall that

$$\sqrt{a^n} = \Big(\sqrt{a^{n-1}} - \frac{1}{2}\int_{t_{n-1}}^{t_n} \bar{\beta}(C_s - \bar{C}^n)_+\Big)_+, \qquad \sqrt{a(t_n)} = \Big(\sqrt{a(t_{n-1})} - \frac{1}{2}\int_{t_{n-1}}^{t_n} \beta(C_s - C)_+\Big)_+.$$

Subtracting both equations and using that the mapping $x \to (x)_+$ is Lipschitz, we obtain

$$\begin{aligned} |\sqrt{a^n} - \sqrt{a(t_n)}| &\le |\sqrt{a^{n-1}} - \sqrt{a(t_{n-1})}| + \frac{1}{2}\int_{t_{n-1}}^{t_n} \big(\bar{\beta}|C - \bar{C}^n| + |\bar{\beta} - \beta|(C_s - C)_+\big)\,\mathrm{d}t \\ &\le |\sqrt{a^{n-1}} - \sqrt{a(t_{n-1})}| + \frac{1}{2}\int_{t_{n-1}}^{t_n} \bar{\beta}\,\big|\bar{C}^n - C^n + \theta_C^n + \rho_C^n\big|\,dt \\ &\quad + \frac{1}{2}\int_{t_{n-1}}^{t_n} \bar{\beta}\,|C(t_n) - C(t)|\,dt + \frac{1}{2}\Delta t C_s |\bar{\beta} - \beta|, \end{aligned}$$

where we have used the decomposition (7.5).

Then, (7.2) yields

$$\Big\|\sqrt{a^n} - \sqrt{a(t_n)}\Big\| \le \Big\|\sqrt{a^{n-1}} - \sqrt{a(t_{n-1})}\Big\| + \Delta t \frac{\|\beta\|_{L^\infty}}{2}\big(\|\bar{C}^n - C^n\| + \|\theta_C^n\| + \|\rho_C^n\|\big) + \frac{\|\beta\|_{L^\infty}}{2}\int_{t_{n-1}}^{t_n} \Big\|\int_t^{t_n} C_t(s)\Big\|\,\mathrm{d}s + \frac{1}{2}\Delta t C_s \mathbb{C}^* h \|\beta\|_{H^1},$$

and using (7.3) we readily obtain the claim. □

Putting together the previous two lemmas we can prove Theorem 15.

Proof of Theorem 15. Using $(\alpha + \beta)^2 \le (1 + \Delta t)\alpha^2 + \big(1 + \frac{1}{\Delta t}\big)\beta^2$ in (7.8) we obtain

$$\Big\|\sqrt{a^n} - \sqrt{a(t_n)}\Big\|^2 \le (1 + \Delta t)\Big\|\sqrt{a^{n-1}} - \sqrt{a(t_{n-1})}\Big\|^2 + \Delta t \mathbb{C}_{10}^2 (\Delta t + 1)\big(\|\theta_C^n\| + h\|C^n\|_{H^1} + h\|C(t_n)\|_{H^1} + \Delta t\|C_t\|_{L^\infty(L^2)} + h\big)^2.$$

And using estimate (7.6) in the above inequality, we have

$$\|\sqrt{a^n} - \sqrt{a(t_n)}\|^2 \le (1 + \Delta t)\|\sqrt{a^{n-1}} - \sqrt{a(t_{n-1})}\|^2 + \mathbb{C}_{10}^2 \Delta t(1 + \Delta t)\Big[\|\theta_C^{n-1}\|^2 + \mathbb{C}_9 \Delta t\Big(\|\sqrt{a^{n-1}} - \sqrt{a(t_{n-1})}\|^2 + \Delta t \int_{t_{n-1}}^{t_n} \|a_t(s)\|^2\,\mathrm{d}s + \tilde{\mathbb{C}}^2 h^2 \|C\|^2_{L^\infty(H^1)} + \frac{\tilde{\mathbb{C}}^2 h^2}{\Delta t}\int_{t_{n-1}}^{t_n} \|C_t(s)\|^2_{H^1}\,\mathrm{d}s + \Delta t \int_{t_{n-1}}^{t_n} \|C_{tt}(s)\|^2_{H^{-1}}\,\mathrm{d}s\Big) + h^2\|C^n\|^2_{H^1} + h^2\|C(t_n)\|^2_{H^1} + \Delta t^2 \|C_t\|^2_{L^\infty(L^2)} + h^2\Big].$$

Adding this inequality to the estimate (7.6), and defining $\mathbb{C}_{11} = \max\{\mathbb{C}_9 + 1, \mathbb{C}_{10}^2\mathbb{C}_9, \mathbb{C}_{10}^2 + \mathbb{C}_9\}$, it results

$$\begin{aligned}\|\sqrt{a^n} - \sqrt{a(t_n)}\|^2 + \|\theta_C^n\|^2 \leq\ & (1 + \mathbb{C}_{11}(\Delta t + \Delta t^2 + \Delta t^3))\Big[\|\sqrt{a^{n-1}} - \sqrt{a(t_{n-1})}\|^2 + \|\theta_C^{n-1}\|^2 \\ & + \mathbb{C}_9\Delta t^2 \int_{t_{n-1}}^{t_n} \|a_t(s)\|^2\,ds + \mathbb{C}_9\Delta t\tilde{\mathbb{C}}^2h^2\|C\|^2_{L^\infty(H^1)} \\ & + \mathbb{C}_9\tilde{\mathbb{C}}^2h^2 \int_{t_{n-1}}^{t_n} \|C_t(s)\|^2_{H^1}\,ds + \mathbb{C}_9\Delta t^2 \int_{t_{n-1}}^{t_n} \|C_{tt}(s)\|^2_{H^{-1}}\,ds \\ & + \mathbb{C}_{11}\left(\Delta t h^2\|C^n\|^2_{H^1} + \Delta t h^2\|C(t_n)\|^2_{H^1} + \Delta t^3\|C_t\|^2_{L^\infty(L^2)} + \Delta t h^2\right)\Big].\end{aligned}$$

Now, $1 + \mathbb{C}_{11}(\Delta t + \Delta t^2 + \Delta t^3) \leq 1 + \mathbb{C}_{12}\Delta t$ with $\mathbb{C}_{12} = \mathbb{C}_{11}(1 + t_F + t_F^2)$. By induction on n and using $1 + \mathbb{C}_{12}\Delta t \geq 1$ we obtain

$$\begin{aligned}\|\sqrt{a^n} - \sqrt{a(t_n)}\|^2 + \|\theta_C^n\|^2 \leq\ & \left(1 + \mathbb{C}_{12}\Delta t\right)^n \Big\{\Big[\|\sqrt{a^0} - \sqrt{a(0)}\|^2 + \|\theta_C^0\|^2\Big] \\ & + \mathbb{C}_9\Delta t^2 \int_0^{t_F} \left(\|a_t(s)\|^2 + \|C_{tt}(s)\|^2_{H^{-1}}\right) ds \\ & + \mathbb{C}_9 t_F\tilde{\mathbb{C}}^2h^2\|C\|^2_{L^\infty(H^1)} + \mathbb{C}_9\tilde{\mathbb{C}}^2h^2 \int_0^{t_F} \|C_t(s)\|^2_{H^1}\,ds \\ & + \mathbb{C}_{11}\Big(h^2\Delta t \sum_{j=1}^{n} \|C^j\|^2_{H^1} + t_F h^2\|C\|^2_{L^\infty(H^1)} + t_F\Delta t^2\|C_t\|^2_{L^\infty(L^2)} + t_F h^2\Big)\Big\}.\end{aligned}$$

Therefore, using the stability bound (7.1), and the fact that $(1 + \mathbb{C}_{12}\Delta t)^n \leq e^{\mathbb{C}_{12}t_n} \leq e^{\mathbb{C}_{12}t_F} =: \mathbb{C}_{t_F}$, the claim follows. □

Proof of Theorem 17. From (7.7),

$$\begin{aligned}\|\theta_C^j\|^2 - \|\theta_C^{j-1}\|^2 + \Delta t\mathscr{B}[\theta_C^j, \theta_C^j] \leq\ & \mathbb{C}_9\Delta t\Big(\left\|\sqrt{a^{j-1}} - \sqrt{a(t_{j-1})}\right\|^2 + \Delta t \int_{t_{j-1}}^{t_j} \|a_t(s)\|^2\,ds \\ & + \tilde{\mathbb{C}}^2h^2\|C\|^2_{L^\infty(H^1)} + \frac{\tilde{\mathbb{C}}^2h^2}{\Delta t} \int_{t_{j-1}}^{t_j} \|C_t(s)\|^2_{H^1}\,ds + \Delta t \int_{t_{j-1}}^{t_j} \|C_{tt}(s)\|^2_{H^{-1}}\,ds\Big),\end{aligned}$$

and adding from 1 to $M = \lceil t_F/\Delta t\rceil$, as we did in the proof of the stability of $\|C^n\|$, we obtain

$$\begin{aligned}\|\theta_C^M\|^2 + \Delta t \sum_{j=1}^{M} \mathscr{B}[\theta_C^j, \theta_C^j] \leq\ & \|\theta_C^0\|^2 + \mathbb{C}_9\Delta t \sum_{j=1}^{M}\Big(\|\sqrt{a^{j-1}} - \sqrt{a(t_{j-1})}\|^2\Big) \\ & + \mathbb{C}_9\Delta t^2\left(\|a_t\|^2_{L^2(L^2)} + \|C_{tt}\|^2_{L^2(H^{-1})}\right) + \mathbb{C}_9\tilde{\mathbb{C}}^2h^2(t_F\|C\|^2_{L^\infty(H^1)} + \|C_t\|^2_{L^2(H^1)}).\end{aligned}$$

Taking into account the coercivity of the bilinear form, stated in Remark 2,

$$\begin{aligned}\mathbb{C}_1\Delta t \sum_{j=1}^{M} \|\theta_C^j\|^2_{H^1} \leq\ & \|\theta_C^0\|^2 + \mathbb{C}_9 M\Delta t \max_{1\leq j\leq M} \|\sqrt{a^{j-1}} - \sqrt{a(t_{j-1})}\|^2 \\ & + \mathbb{C}_9\Delta t^2(\|a_t\|^2_{L^2(L^2)} + \|C_{tt}\|^2_{L^2(H^{-1})}) + \mathbb{C}_9\tilde{\mathbb{C}}^2h^2(t_F\|C\|^2_{L^\infty(H^1)} + \|C_t\|^2_{L^2(H^1)})\end{aligned}$$

and using the estimate of Theorem 15 and Lemma 20, we arrive at

$$\mathbb{C}_1\left(\Delta t \sum_{j=1}^{M} \|\theta_C^j\|^2_{H^1}\right)^{1/2} \leq \|\theta_C^0\| + \mathbb{C}^*_{t_F}[\|C^0 - C(0)\| + \|\sqrt{a^0} - \sqrt{a(0)}\|] + \mathbb{C}^*_{t_F}(h + \Delta t),$$

which is the desired assertion. □

8. Conclusions

We have presented a thorough investigation of a mathematical model for the dissolution of a drug dispersed throughout a polymeric matrix and the diffusion of the dissolved drug inside it. The model applies to a wide range of polymeric devices, and does not hinge upon an assumption of the dissolution being fast or slow relative to the diffusion of the dissolved drug. We have deduced the model, which is a coupled nonlinear system. It consists of a parabolic equation for the dissolved

drug and an ordinary differential equation for the solid drug, that is assumed to be distributed in the whole domain into microspheres which can differ in size. We have analyzed some qualitative properties of the problem such as existence, uniqueness and regularity of solutions. Uniqueness and regularity are proved when the initial concentration of dissolved drug is below saturation. We have also proved that multiple solutions appear when the initial concentration of dissolved drug is above the saturation, and there are no solid particles at time $t = 0$.

We have proposed and analyzed a fully discrete finite element method for solving this problem, and proved optimal a priori error estimates in $L^\infty(L^2)$ and in $L^2(H^1)$ for the concentration of dissolved drug, and in $L^\infty(L^2)$ for the area of solid particles per unit volume. These estimates hinge upon the regularity results previously obtained. We present some simulations that illustrate on qualitative as well as quantitative properties of the solutions. We computed the dissolution and diffusion of Progesterone in a CIDR device, and compared with laboratory experiments, observing an excellent agreement when measuring the amount of released drug at different time instants.

From the applications point of view, it is desirable that the release of drug per unit time is as constant as possible, staying below the toxicity level and above the minimum effective dose. The numerical method developed and tested in this article is an essential building block for solving a shape optimization problem to address this goal of paramount importance for designers. Another goal of this shape optimization problem is to have, at the end of the application procedure, a minimal amount of residual drug, in order to minimize production costs and negative consequences for the environment.

The next step regarding the modeling of drug releasing devices involves dealing with erodible and biodegradable polymers, which would release all the drug and would dematerialize at the end of the treatment, without need of removal. This entails leading with a moving or free boundary, which changes as the domain erodes. We expect that this article sets the basis for the analysis and simulation of these more complicated problems.

Acknowledgments

This work was partially supported by CONICET through grants PIP 112-200801-02182, PIP 112-2011-0100742, by Universidad Nacional del Litoral through grant CAI+D 501 201101 00476 LI, and by Agencia Nacional de Promoción Científica y Tecnológica, through grants PICT-2008-0622, PICT-2012-2590 (Argentina).

References

[1] J. Siepmann, F. Siepmann, Mathematical modeling of drug delivery, Int. J. Pharm. 364 (2008) 328–343.
[2] J. Siepmann, N.A. Peppas, Modeling of drug release from delivery systems based on hydroxypropyl methylcellulose (HPMC), Adv. Drug Delivery Rev. 48 (2001) 139–157.
[3] Encyclopedia of Controlled Drug Delivery, Volumes 1–2, John Wiley & Sons, 1999.
[4] A.K. Bajpai, S.K. Shukla, S. Bhanu, S. Kankane, Responsive polymers in controlled drug delivery, Prog. Polym. Sci. 33 (11) (2008) 1088–1118.
[5] N.R. Leitman, D.C. Busch, D.J. Wilson, D.A. Mallory, M.R. Ellersieck, M.F. Smith, D.J. Patterson, Comparison of controlled internal drug release insert-based protocols to synchronize estrus in prepubertal and estrous-cycling beef heifers, J. Anim. Sci. 87 (2009) 3976–3982.
[6] M.J. Rathbone, C.R. Bunt, C.R. Ogle, Reengineering of a commercially availiable bovine intravaginal insert (CIDR insert) containing progesterone, J. Control. Release 85 (2002) 105–115.
[7] M.I. Cabrera, J.A. Luna, R.J.A. Grau, Modeling of dissolution-diffusion controlled drug release from planar polymeric systems with finite dissolution rate and arbitrary drug loading, J. Membr. Sci. 280 (2006) 693–704.
[8] I.M. Helbling, J.C.D. Ibarra, J.A. Luna, M.I. Cabrera, R.J.A. Grau, Modeling of drug delivery from erodible and non-erodible laminated planar devices into finite external medium, J. Membr. Sci. 350 (2010) 10–18.
[9] M.I. Cabrera, R.J.A. Grau, A generalized integral method for solving the design equations of dissolution-diffusion controlled drug release from planar, cylindrical and spherical matrix devices, J. Membr. Sci. 293 (2007) 1–14.
[10] Roger Temam, Navier–Stokes Equations: Theory and Numerical Analysis, North Holland, 1977.
[11] D. Andreucci, C. Verdi, Existence, uniqueness, and error estimates for a model of polymer crystallization, Adv. Math. Sci. Appl. 5 (1995) 391–409.
[12] J.I. Díaz, I. Stakgold, Mathematical aspects of the combustion of a solid by a distributed isothermal gas reaction, SIAM J. Math. Anal. 26 (1995) 305–328.
[13] D. Gilbarg, N.S. Trudinger, Elliptic Partial Differential Equations of Second Order, Springer-Verlag, 2001.
[14] L.C. Evans, Partial Differential Equations, American Mathematical Society, 1998.
[15] P. Grisvard, Elliptic Problems in Nonsmooth Domains, Pitman, 1985.
[16] S. Funken, D. Praetorius, P. Wissgott, Efficient implementation of adaptive P1-FEM in MATLAB, Comput. Methods Appl. Math. 11 (2011) 460–490.
[17] T. Rahman, J. Valdman, Fast MATLAB assembly of FEM matrices in 2D and 3D: Nodal elements, Appl. Math. Comput. 219 (2013) 7151–7158.
[18] S. Márquez Damián, R.N. Mariano, N.M. Nigro, R.J.A. Grau, Development and validation of a numerical model for controlled intravaginal drug releasing devices, in: Mecánica Computacional Vol XXX, págs. 3439–3448, 1–4 Noviembre 2011, Rosario, Argentina.
[19] C. Geuzaine, J.-F. Remacle, Gmsh: a three-dimensional finite element mesh generator with built-in pre- and post-processing facilities, Internat. J. Numer. Methods Engrg. 79 (11) (2009) 1309–1331.
[20] D. Braess, Finite Elements. Theory, Fast Solvers, An Applications in Solid Mechanics, second ed., Cambridge University Press, 2001.
[21] S.C. Brenner, L.R. Scott, The Mathematical Theory of Finite Element Methods, second ed., Springer, 2002.
[22] P.G. Ciarlet, The Finite Element Method for Elliptic Problems, North-Holland, New York, 1978.